Pisco Med Publishing

Effect of Olefins on Desulfurization Mechanism of Thiophene Adsorption on Active Site Species of Mesoporous Molecular Sieve Al-MCM-41

Hongshen Wang
Jiangsu Tianci Energy Chemical Co., Ltd., wanghs@piscomed.com

Abstract: The Al-MCM-41 and Molecular Sieve with different aluminum loadings were prepared by post grafting method. Characterization of Molecular Sieves by XRD, N2 Adsorption- Desorption NH3-TPD, Py-FTIR and other methods. Evaluation of Thiophene Adsorption Performance by Fixed Bed. By correlating the thiophene adsorption capacity of molecular sieves with the acid properties and texture properties of molecular sieves, examine the influence of olefin presence on Al-MCM-41 and Adsorption and Desulfurization Mechanism of Active Site Species. The results show that the introduction of aluminum species produces B-type acid center, as well as two types of L acid center, L1 and L2. The introduction of low content aluminum species is beneficial to the formation of B-type acid centers and L1-type acid centers, while the introduction of high content aluminum species is beneficial to the formation of L2-type acid centers. Among them, L2-type acid center has the best adsorption effect on Thiophene. Olefins and thiophenes undergo competitive adsorption and catalytic conversion reactions at B and acid centers, and catalytic conversion reactions dominate. The existence of L2 acid center promotes the catalytic conversion reaction on the B acid center, and the generated macromolecular sulfide replaces thiophene to be adsorbed on the molecular sieve acid active center, thus improving the saturated sulfur adsorption capacity of Al-MCM-41 molecular sieve.

Keywords: Al-MCM-41; Molecular Sieve; Thiophene; Olefin; Acid Center; Adsorption Desulfurization Mechanism

Removal of thiophene sulfide (70%) accounting for about the total sulfur content in FCC gasoline has become a key factor affecting clean gasoline production [1]. The traditional hydrodesulfurization process results in serious loss of gasoline octane number and yield drop due to excessive hydrogenation. The selective adsorption desulfurization technology has good development prospects due to mild reaction conditions, no hydrogen consumption and no loss of gasoline octane number [2-4]. However, a large number of olefins (AB. 20%, Volume Fraction) Severe Competitive Adsorption of Thiophene with Trace Amounts on Active Center of Adsorbent [5-6], which restricts industrial application of adsorption desulfurization technology.

Clear understanding and directional construction of adsorption active centers are the key to overcome the above problems. Researchers have done a lot of work on microporous aluminosilicate molecular sieves. Our research group [7-9] taking modification, Y and molecular sieve as research objects discovers through in-situ infrared technology that L and acid centers related to metal species are more conducive to adsorption of thiophene sulfide. Schallmoser et al. [10] takes ZSM-5 as research object, proposes the mechanism of alkene with b, acid active center Based on the carbocation mechanism. Richardeau et al [11] and Shi et al [12] taking HFAU, NaY and LaNaY molecular sieves as research objects found that b and acid center lead to the catalytic conversion reaction between alkene and thiophene, respectively from the angle of experiment and theory. However, taking microporous aluminosilicate molecular sieve as the research object inevitably has the following problems: microporous aluminosilicate molecular sieve will simultaneously form aluminum species with different chemical forms in the process of synthesizing molecular sieve, adsorption between different aluminum species has great difference and mutual influence. How to distinguish the role of different chemical forms of aluminum species in adsorption desulfurization becomes a challenge.

Silicon-based mesoporous molecular sieve does not have any active centers. The introduction of aluminum species into the silicon hydroxyl or skeleton structure on the molecular sieve surface can realize the effective construction and adjustment of different active centers. Therefore, modified silica-based mesoporous molecular sieves bring new opportunities for further understanding the adsorption behavior of thiophene sulfides on the active center of adsorbent. Selvaraj, et al. [13] and Wang, et al. [14] adopted AlMASNMR to technically analyze the chemical forms of different aluminum species in Al-MCM-41 and the chemical species of different chemical forms were effectively associated with the L acid center and the B acid center. Hu , et al [15] using TMP, TMPO and acetone as probe molecules investigated Al-SBA-15 acid properties and adsorption capacity of molecular sieves and found the phenomenon of different acid strength of molecular sieves detected by different probe molecules. Gurinov, et al[16] taking Al-SBA-15 and Molecular Sieve as the research objects, combined NNMR and FT-IR technology examines the adsorption behavior of different acid active centers on Pyridine. It is found that the adsorption capability of active centers on pyridine in different chemical forms is different. The above studies show that the adsorption capacity of the molecular sieve is closely related to the chemical form of the active center. In the combined experiment, the number of thiophene sulfide molecules adsorbed by the active center of the molecular sieve is significantly lower than the theoretical value [17], and it is speculated that the aluminum species of different chemical forms are Optimal adsorption of thiophene sulfide forms. However, there are few reports on the systematic investigation of adsorption behavior of thiophene sulfide by active centers of aluminum species with different chemical forms (especially adsorption and removal of thiophene sulfide) in the presence of olefin.

In this project, aluminum modified MCM-41 molecular sieve, uses XRD, N2 adsorption-desorption, NH 3-TPD, Py-FTIR and other technologies to characterize and analyze the texture and acid properties of molecular sieve. Evaluation of desulfurization performance of molecular sieves through fixed bed dynamic adsorption experiments and extraction experiments. Joint, GC-SCD and Technical Investigation of Influence of Olefins on Desulfurization Performance of Molecular Sieves. The formation rules of acid active centers in different aluminum species were summarized, and the mechanism of their action in the process of thiophene sulfide removal was analyzed, which provided guidance for the development of high-efficiency desulfurization adsorbents.

1. Experimental Section

1.1 Raw Materials and Reagents

MCM-41 Molecular Sieve (Nankai University Catalyst Factory), aluminium trichloride, Anhydrous Ethano, n-Octane (Analytical Purity, National Pharmaceutical Group Chemical Reagents Co., Ltd.), Thiophene, Pyridine, 1- Hexen (Imported Analytical Purity, Bailiwei Chemical Reagents Co., Ltd.).

1. 2 Preparation of Adsorbent and Simulated Oil

AlCl3 was loaded onto MCM-41 molecular sieve by post grafting method to prepare Al-MCM-41 molecular sieve with different aluminum content. The specific process is as follows: Add MCM-41 Molecular Sieve to Different Concentrations of $AlCl_3$- Stir in Ethanol Solution 10h,Filter with Anhydrous Ethanol, Wash, Place Product in Vacuum Drying Cabinet 100℃ Dry Under 10h. After that, the molecular sieve samples with different aluminum contents were marked as Al-MCM-41 (X), X and were prepared in a muffle furnace 500℃ lower roasting 6h. Thiophene Dissolved in n-Octane, configured as Model Oil with Sulfur Content of 300 μ G/G, noted as MO-1; Thiophene as Solute, 1- Hexene and n-octane as Solvents, Configured as 300 μ G/G Model Oil with Sulfur Content and Containing 20%1- Hexene, Noted as MO-2.

1.3 Characterization of Adsorbents

The physical parameters of molecular sieve samples are respectively determined by X and X ray diffractometer (Japan Science Co., Ltd.), ASAP2020 type physical adsorption instrument (American Mike Company) and Inductively Coupled Plasma Emission Spectrometer (American Thermoelectric Company) Determination. Refer to Reference [18-19] for specific process. The acid properties of molecular sieve samples are determined by AutoChemII2920 type chemisorber (American Mike Company) and Fourier Transform Infrared Spectrometer(United States, PE and Company)

Determination. Refer to Reference [19-20]for specific process.

1.4 Desulfurization Performance Evaluation

Dynamic adsorption experiment on fixed bed reactor. Fixed bed reactor built by research group, consists of metering pump, pressure gauge, temperature controller, flowmeter, reactor (Quartz Tube, 6mm× 4mm× 50cm) and heater. Before the experiment, activate the sample under the conditions of N_2 atmosphere, 400℃ for 6h, dynamic adsorption desulfurization experiment under ambient temperature, adsorbent sample dosage is 1g, bed height is about 15cm, simulated oil volume space velocity is $5h^{-1}$, every 20min Oil sample analysis at the reactor outlet. Refer to references [21] for calculation method of sulfur adsorption capacity of adsorbent. Sulfide components in oil products are detected by gas chromatography-sulfide light detector (GC-SCD, PE Company of the United States). Refer to reference [8] for the specific process. The total sulfur content of the oil sample was measured by WK-2D micro coulometer (Jiangsu Jiangfen Instrument Company). The extraction experiment was carried out on the deactivated adsorbent. The specific process was as follows: drying the deactivated adsorbent sample at 40℃, dissolving with 40mL NaOH(2mol/L), extracting with 5mL toluene, centrifuging, and taking the supernatant for GC-SCD analysis.

2. Results and Discussions

2.1 Characterization of Texture Properties of Molecular Sieves

Fig. 1 is XRD spectrum of Al-MCM-41 molecular sieves with different aluminum contents, and Table 1 is physical property parameters of Al-MCM-41 molecular sieves with different aluminum contents. From the diagram 1 (A), we can see all samples are in 1. 0°-2.2° . There are three characteristic diffraction peaks, respectively correspond to (100), (110) and (200) crystal plane of molecular sieve, indicating that molecular sieve has regular two-dimensional hexagonal pore structure. Although there is still a diffraction peak, corresponding to the above crystal plane in the aluminum modified molecular sieve, the positions of the diffraction peaks are respectively from 1.24°, 1.87° and 2.12° Offset to small angle 1.13°, 1.80° and 2.01, indicating a decrease in crystallinity and order of the sample. According to Table 1, with the increase of the content of introduced aluminum species, the plane spacing D and unit cell parameter a0 of diffraction peaks on the (100) crystal plane of the molecular sieve become larger, which is due to the replacement of silicon atoms in the molecular sieve framework (Si-O-Si) by aluminum species to form Si-O-Al structure, distorting the pore structure. When aluminum species are excessively introduce (see Al-MCM-41(10)), the plane spacing D and unit cell parameter a0 of the diffraction peaks on the (100) crystal plane of the molecular sieve are obviously reduced, which indicates that the surplus aluminum species act with silicon hydroxyl (Si-OH) on the surface of the molecular sieve to block the pore channels. From the graph 1 (B), it is known that all samples have a wide diffraction peak, located near 23° which is generally classified as amorphous SiO_2. No other characteristic diffraction peaks were found in all samples, indicating that the introduced aluminum species are highly dispersed in the molecular sieve.

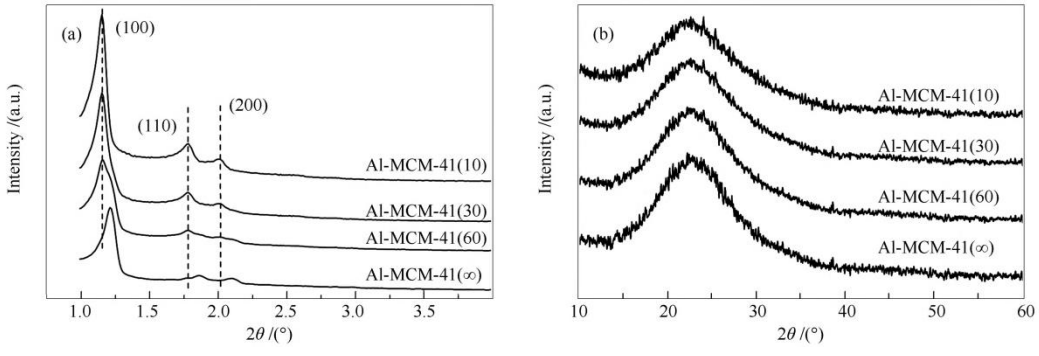

Figure1 XRD patterns of the Al-MCM-41 samples

(a): low-angle; (b):wide-angle

Table 1 Textural parameters of the different Si/Al ratio Al-MCM-41 samples

Sample	A_{BET} /($m^2 \cdot g^{-1}$)	A_{mic} /($m^2 \cdot g^{-1}$)	A_{meso} /($m^2 \cdot g^{-1}$)	v_p /($cm^3 \cdot g^{-1}$)	Average pore diameter d/nm	a_0/nm	w/% (Al)
Al-MCM-41(∞)	1069.3	12.3	1057	1.0	2.79	3.22	–
Al-MCM-41(60)	1067.4	12.5	1054.9	0.9	2.82	3.26	0.70
Al-MCM-41(30)	1063.1	12.8	1050.3	1.0	2.83	3.27	1.41
Al-MCM-41(10)	1046	9.6	1036.4	0.85	2.70	3.12	3.99

w/% (Al): actual Al content in samples which is tested by ICP-MS

The N2 adsorption-desorption isotherm and pore size distribution of Al-MCM-41 samples with different aluminum contents are shown in Figure 2. From figure 2 we can see all samples are of IV type N_2 adsorption - desorption isotherm and present H1 type hysteresis ring, indicating that the introduction of aluminum species has not destroyed the mesoporous pore structure. All samples are in $P/p/p_0 \approx 0.30-0.40$ and $P/P_0 \approx 0.42-1$. There are two different hysteresis loops,corresponding to two different N_2 capillary condensation phenomenon, indicating that there are two different pore sizes. From the aperture distribution map, $P/P_0 \approx 0.30-0.40$ Capillary condensation at 40 corresponds to about 2. 6nm Pore Hole, and $P/p/p_0 \approx 0.42-1.0$ Capillary condensation at 0 corresponds to about 3.6, and with a pore size of about 2.6 nm. In addition, with the increase of aluminum content, molecular sieve and N_2 adsorption capacity gradually decreases, $P/P_0 \approx 0.42-1.0$ The hysteresis loop at 0 gradually widens. Combined with the specific surface area and pore volume of the molecular sieve in Table 1, the aluminum content decreases with the increase of the aluminum content, indicating that the introduced aluminum species acts on the surface silicon hydroxy group to block the pores.

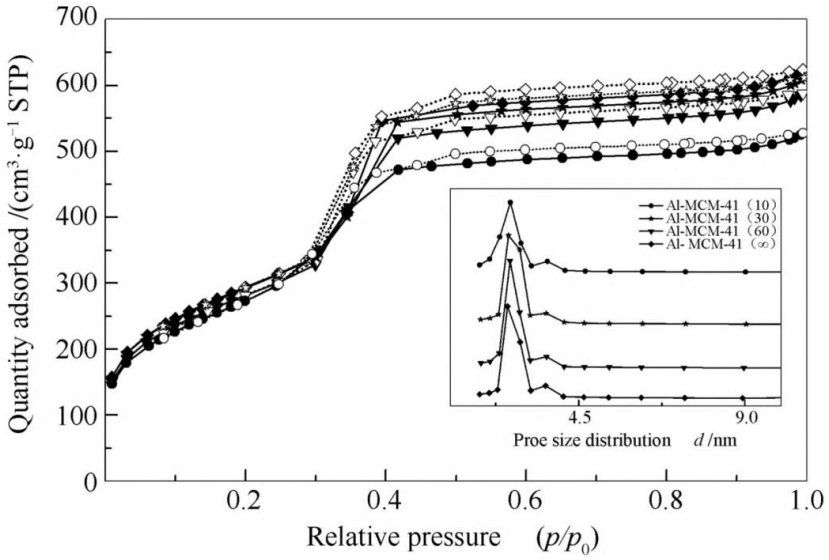

Figure2 Nitrogen adsorption-desorption isotherms and BJH pore size distributions of the Al-MCM-41samples

◆: Al-MCM-41(∞)adsorption; ◇:Al-MCM-41(∞)desorption;

:Al-MCM-41(60)adsorption; :Al-MCM-41(60)desorption;

★:Al-MCM-41(30)adsorption; ☆:Al-MCM-41(30)desorption;

●:Al-MCM-41(10)adsorption;○:Al-MCM-41(10)desorption

2.2 Discrimination of Molecular Sieve Active Species

Fig. 3 is NH3-TPD spectra of Al-MCM-41 samples with different aluminum contents. From the graph 3 we can see

all samples have three NH 3 desorption signal peak. The desorption signal peak of 186－192℃ corresponds to the desorption signal peak of weak acid center(WA), 235－256℃ corresponds to the desorption signal peak of medium-strength acid center(MS), 317－342℃ corresponds to strong acid center (SA). Further analysis found that with the increase of the introduction of aluminum species, the acid content of the three strength acid centers in the molecular sieve all increased to varying degrees, the total acid content of the molecular sieve increased. Al-MCM-41 (∞) Weak Acidity in Molecular Sieve, and MA and Amount of Acid Contributed. In Al-MCM-41(60) molecular sieve, the acid content of SA is the main, followed by that of MA, and the acid content of WA is the least. The ratio of acid centers of Al-MCM-41(30) and Al-MCM-41(60) molecular sieves is basically the same, but the total amount of acid is greatly increased. The total acid content of Al-MCM-41(10) is not much higher than that of Al-MCM-41(30), but the acid content ratio between different acid centers changes obviously. MA is the main acid content in Al-MCM-41(10), WA is the second, and SA is the least.

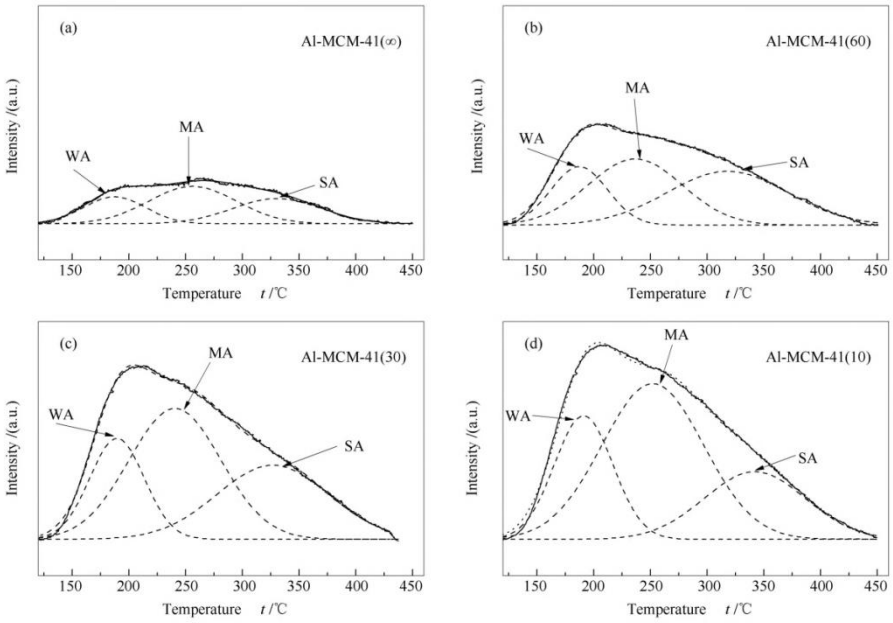

Figure3 NH_3-TPD patterns and Gaussian fitting profiles of the Al-MCM-41samples

—: actualcurve; ---- :fitcurves

Figure 4 shows the infrared spectrum of pyridine in different aluminum content Al-MCM-41 samples(Py-FTIR). It is known from the reference [22] that aluminum species introduced by post grafting exist in different coordination chemical forms (see figure 5). Six-coordinated aluminum species cannot adsorb pyridine due to coordination saturation. Therefore, the characteristic absorption peak corresponding to it cannot be observed in Figure 4. All samples in Figure 4 have characteristic absorption peaks with a wavenumber of 1545cm^{-1}, which is produced by the interaction between the pyridine molecule and the silicon-aluminum bridge hydroxyl hydrogen bond (PyH+). Silicon-aluminum bridge hydroxyl group exists in the four-coordinated aluminum species, therefore, molecular sieve, B and acid center exists in Tetra-coordinated Aluminum Species Chemical Form. Contrast Map 4(A) and 4(B) we can see that 400℃ Desorption 1545cm $^{-1}$ Characteristic Peak Intensity Significantly Lower than 150℃ Desorption Peak Intensity. Combied Diagram 3 we can see that in sample B is weak acid center. Further comparison of different samples shows that 1545cm^{-1} the peak intensity of the characteristic peak increases first and then decreases with the increase of aluminum content. It can be seen from Table 2 that when the Si/Al ratio is 30, the proportion of B t0>s in the molecular sieve reaches the maximum, indicating that when the low content of aluminum species is introduced, the aluminum species is easy to enter the molecular sieve framework to form the B acid centers in the form of four coordination. After a certain amount of aluminum species is introduced, aluminum species cannot continue to enter the molecular sieve framework, but the interaction with surface

silicon hydroxyl groups increases the number of L acid centers, resulting in a relative decrease in the proportion of B acid centers.

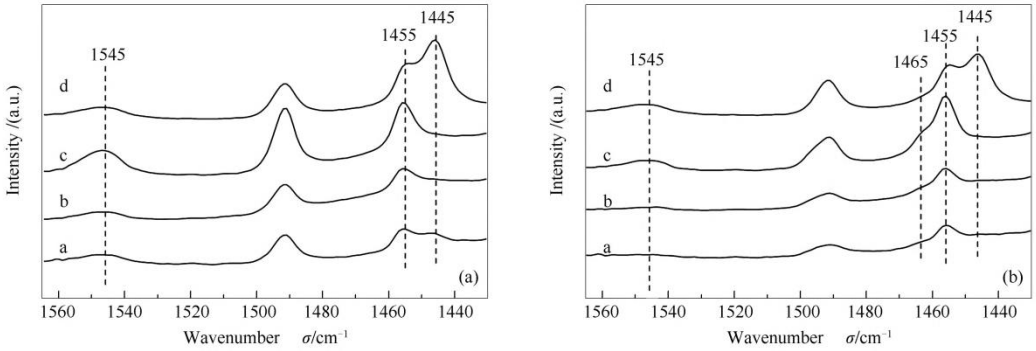

Figure4 Py-FTIR characterization of the Al-MCM-41 samples

(a):150℃ of desorption temperature; (b):400℃ of desorption temperaturea: Al -MCM-41(∞); b: Al-MCM-41(60); c:Al-MCM-41(30); d:Al-MCM-41(10)

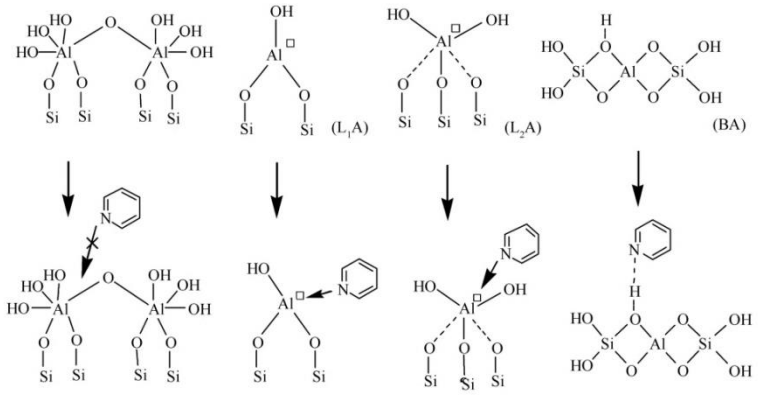

Figure5 Type of acid active centers in Al-MCM-41 samples

BA: Brnsted acid site; L_1A and L_2A: type1 and type2 Lewis acid site

Except 1545cm^{-1} characteristic peak related to B-acid, 1455 cm^{-1} characteristic peak was observed in pyridine infrared spectra of all samples, and 1445 cm^{-1} characteristic peak was also observed in Al-MCM-41(10) and Al-MCM-41(∞) samples. These two characteristic peaks are usually produced by pyridine and L-acid center action or surface silicon hydroxyl action. The aluminum species in the three-coordinate and penta-coordinate forms in Figure 5 are important sources of L acid centers. Since the three-coordinated aluminum species has stronger electron interaction with the surface silanol, the tri-coordinated aluminum species is more easily formed and should be attributed to the L1-type acid center, and the pyridine interaction (PyL1) produces a 1455 cm^{-1} characteristic peak.[23]The five-coordinate aluminum species has weaker interaction with the surface silanol, and its larger structure leads to greater steric hindrance. Therefore, the five-coordinate aluminum species is difficult to form and should be attributed to the L2 acid center and pyridine. Effect (PyL2) produces a characteristic peak of 1445 cm^{-1}[24].

Comparing Figure 4(a) with Figure 4(b), it is known that all samples at 400 °C desorption, the peak intensity of the 1455 cm^{-1} characteristic peak in all samples is basically unchanged. Al-MCM-41 (10) and Al-MCM-41 (∞) Medium 1445cm^{-1} Characteristic Peak Intensity Attenuated. The combination diagram 3 shows that the type acid center L_1 is a medium-strong acid center, L_2 type acid center is a medium-strength acid center. Further comparison of different samples

shows that 1455 cm^{-1} characteristic peak intensity shows a trend of increasing first and then decreasing with the increase of aluminum content. Combination Table 2 it is known that Molecular Sieve with Si/Al Ratio of 60, L_1 Largest Proportion of Type Acid Center, indicatings L_1 type acid center can be easily formed at very low aluminum content. The 1445 cm-1 characteristic peak in Al-MCM-41 (∞) disappeared after the introduction of the aluminum species due to the interaction of the introduced aluminum species with the surface silanol to form the L1 type acid center. Compared with Al-MCM-41 (30) and Al-MCM-41 (60), the 1445 cm^{-1} characteristic peak reappeared in the Al-MCM-41 (10) sample, and the L2 associated with the 1445 cm-1 characteristic peak. The proportion of acid center is significantly larger than other acid centers, indicating that L2 type acid centers are more likely to form when high aluminum species are introduced. In addition, a characteristic absorption peak of 1465 cm-1 was also observed in the Al-MCM-41 (30) and Al-MCM-41 (60) sample spectra (Fig. 4(b)), which is generally considered to be from B. The L1 type acid center adjacent to the acid center is formed by the action of pyridine [13, 24], and the acid center may be formed by dehydration of a part of the B acid center.

Table 2 Proportion of active sites in Al-MCM-41 samples

Sample	$B/(B+L_1+L_2)$	$L_1/(B+L_1+L_2)$	$L_2/(B+L_1+L_2)$
Al-MCM-41(∞)(150 ℃)	0.41	0.53	0.06
Al-MCM-41(60)(150 ℃)	0.38	0.62	0
Al-MCM-41(30)(150 ℃)	0.53	0.47	0
Al-MCM-41(10)(150 ℃)	0.16	0.27	0.57
Al-MCM-41(∞)(400 ℃)	0.26	0.74	0
Al-MCM-41(60)(400 ℃)	0.27	0.73	0
Al-MCM-41(30)(400 ℃)	0.26	0.74	0
Al-MCM-41(10)(400 ℃)	0.16	0.30	0.54

note: proportion of active sites are calculated from the peak area of Py-FTIR spectra by emeis's method[25]

2.3 Evaluation of Adsorption Desulfurization Performance

Al-MCM-41 samples with different aluminum contents carry out dynamic adsorption experiments on MO-1 simulated oil, extract the saturated samples, and carry out GC-SCD detection and analysis on the extract. The results are shown in Figure 6. Figure 6 shows that samples with different aluminum contents have certain adsorption capacity for thiophene. With the increase of aluminum content, saturated sulfur adsorption capacity of the sample (SAC) and penetrating sulfur adsorption capacity (BAC , 10 μ G/G Sulfur content as penetration point) increased. Peak intensity of thiophene signal in sample extract increased. According to the texture and acid properties of the samples, aluminum modification, Al-MCM-41 and the maximum specific surface area difference between molecular sieve and molecular sieve raw powder is 23.4m2 /g (Less than 2%), maximum aperture difference 0.09nm(3.2%), and the specific surface area and pore volume decrease with the increase of aluminum content. Type of acid centers among different samples, the relative proportion of different acid centers and the total amount of acid are greatly different. Therefore, the real reason for the difference in desulfurization performance of the samples lies in the difference in acid properties between the samples. The texture properties have less influence.

From the graph 6 (B) we know that no macromolecular sulfide signal was detected in all extracted samples,indicating that an active site favorable for thiophene adsorption has been constructed. By Analyzing Chart 6(C) and 6(D), we know that Al-MCM-41 (60), Al-MCM-41 (30) and Al-MCM-41 (10) compared with Al-MCM-41 (∞) of BAC and Al-MCM-41 increased respectively, 37.5%, 56.3% and 119%, and SAC have been increased by 3. 8%, 7.4% and 17.8%. Combined with the acid properties of the sample, it can be seen that Al-MCM-41(60) has a greater increase in the total acid amount than Al-MCM-41(∞), and the increased acid amount is mainly L1 type acid center (the proportion of L1 type acid center increases by 9%), while the sample has a limited effect on increasing the sulfur adsorption capacity of thiophene, indicating that L1 type acid center has certain adsorption capacity for thiophene, but the adsorption capacity is not strong. The total acid content of Al-MCM-41(30) is higher than that of Al-MCM-41(60), and the acid content of B acid center is mainly increased (the proportion of B acid center is increased by 15%), but Al-MCM-41(30) is only increased by 13% compared with Al-MCM-41(60). 6% BAC and 3.5% SAC indicates that the B acid center has a certain adsorption

capacity for thiophene, and the adsorption capacity of B acid center for thiophene is slightly weaker than that of L1 acid center. Al-MCM-41 (10) Compared with Al-MCM-41 (30) Slightly Increased in Total Acid Amount,Larger Changes in Type and Proportion of Acid Centers (L 2 Up to 57%). At the same time, Al-MCM Al-MCM-41(10) Compared with Al-MCM Al-MCM-41(30) Sample, BAC has lifted 40%, SAC has lift 9.7%, indicating that the L2 acid center has the ability to adsorb thiophene, and the L2 acid center's ability to adsorb thiophene is significantly stronger than L1 acid center.

Different Aluminum Content, Al-MCM-41 and Sample Pair MO-2 Simulated Oil Dynamic Adsorption Experiment. Results are sgown in Figure 7. As can be seen from fig. 7, with the increase of aluminum content, the BAC of Al-MCM-41 sample to thiophene gradually decreases and SAC gradually increases. But the contrast graph 6 and graph 7 shows that compared with the experiment without olefin, the sample's BAC and significant decrease of thiophene in the presence of olefin (Si/Al ratio ∞, 60, 30 and 10 sample decreases by 88. 1%, 94.2%, 95.1% and 96.8%), Thiophene, SAC. And There is a certain degree of improvement (Si/Al ratio ∞, 60, 30 and 10 sample increases of 24. 6%, 25.1%, 30.4% and 25.9%). Based on the competitive adsorption mechanism between 1-hexene and thiophene, it can be explained that the Al-MCM-41 molecular sieve BAC is significantly lower than that without olefin in the presence of olefin. However, the corresponding sample SAC should be significantly lower than when there is no olefin, which is contrary to the experimental results. Therefore, simple competitive adsorption does not effectively explain the effect of olefins on the adsorption and desulfurization performance of Al-MCM-41 molecular sieves.

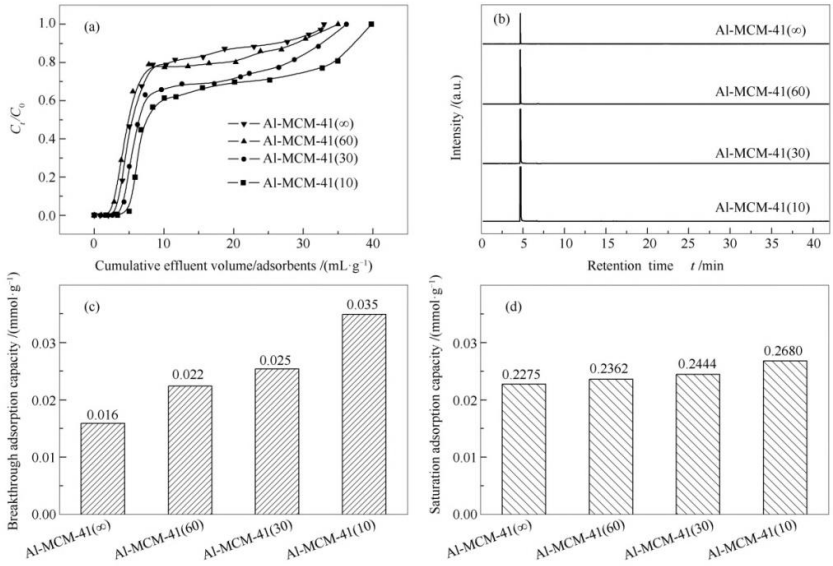

Fig. 6 dynamic adsorption curve (a) of MO-1, GC-SCD spectrum (b) of extraction liquid, penetrating adsorption sulfur capacity (c) and saturated adsorption sulfur capacity (d) of Al-MCM-41 samples with different aluminum contents

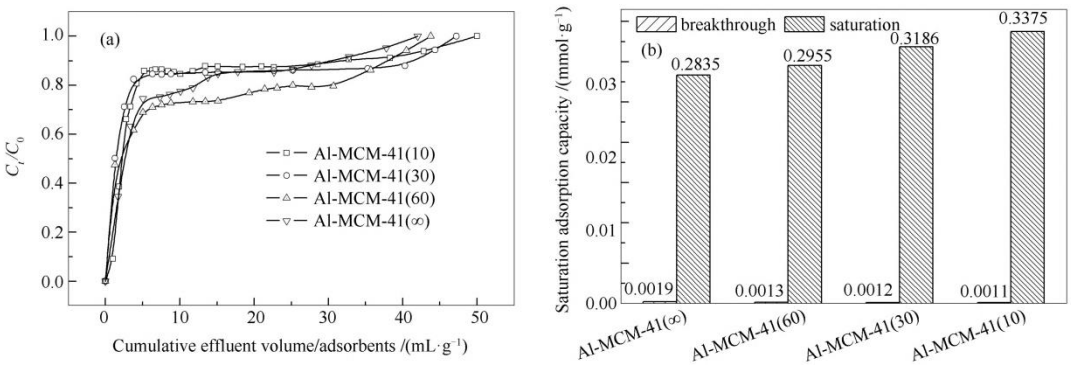

Figure7 Breakthrough curves(a) and sulfur adsorption capacity (b) of the MO-2modeloilon the Al-MCM-41 samples

In order to explore the real reason for the effect of olefins on the removal of thiophene from molecular sieves, the oil samples were taken at different time intervals in the MO-2 simulated oil dynamic adsorption experiment for GC-SCD analysis, and the product distribution map of sulfides at different time periods was obtained. See Figure 8 for details. From figure 8 we can see all oil samples have been detected, C6- thiophene, C12- thiophene macromolecular sulfide. The higher the aluminum content is, the higher the proportion of macromolecular sulfide in the oil sample, indicating that thiophene and olefin undergo catalytic conversion reaction inside the molecular sieve. Combine<rt1> with Py-FTIR characterization results, it can be seen that only the B acid center exists in all samples. It is presumed that the B acid center is the active center of thiophene catalytic conversion reaction. Combined carbocation mechanism [10] adsorbed on B and acid center 1- hexene protonated to form two protonated products, thiophene combined with olefin protonated products to form four C6 - thiophene sulfide (see Figure 9). In addition, the product distribution of all oil samples in graph 8 shows a trend of decreasing the proportion of macromolecular sulfide in oil samples, with the increase of accumulated effluent, this may be due to adsorption of macromolecular sulfide on B and acid active center and caused by the fact that the catalytic conversion reaction cannot continue.

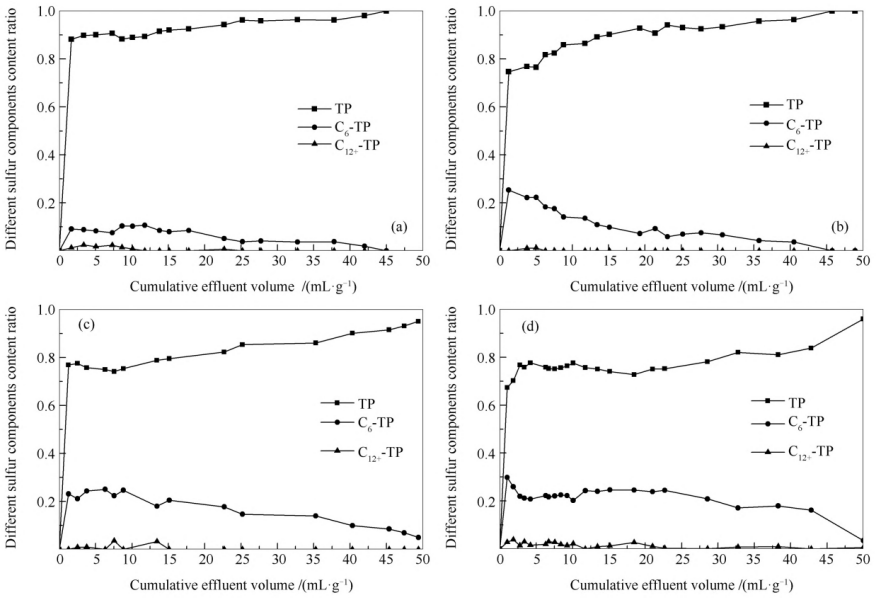

Figure8 Products distribution map of oil samples from the MO-2adsorption tests

(a): Al-MCM-41(∞); (b):Al-MCM-41(60); (c):Al-MCM-41(30); (d):Al-MCM-41(10)

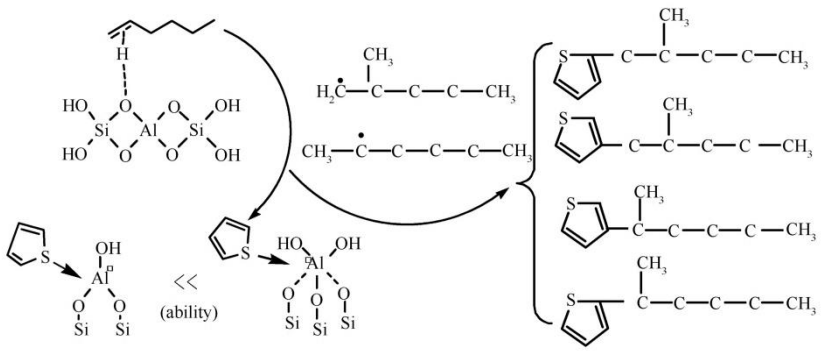

Figure9 Possible reaction mechanism of 1-hexene and thiopheneon the acid active site

The adsorbent sample with saturated adsorption in the MO-2 adsorption experiment was subjected to extraction experiments, and the extract was subjected to GC-SCD analysis. The results are shown in Fig. 10. From Fig. 10 we can see thiophene, C6 - thiophene and C12- thiophene and other sulfides. The larger the proportion of macromolecular sulfides detected in samples with higher aluminum content. However, it can be seen from the figure 4 that Al-MCM-41 (30) is significantly stronger than Al-MCM-41 (10), Al-MCM-41 (10) with A and B and acid L-MCM l-MCM-41(30) not available 1445cm－1 characteristic peak. Therefore, it is presumed that the catalytic conversion of thiophene is not only related to B and acid center, but also related to L2 type acid center. It shows that the L2 acid center is rich in a large amount of thiophene, which promotes the catalytic conversion reaction between thiophene and olefin in the B acid center. the synergistic catalysis between the two is obviously stronger than the single B acid center catalysis. The adsorption of macromolecular sulfide substituted thiophene to the active site is the real reason why the saturated sulfur adsorption capacity of adsorbent pair MO-2 is higher than MO-1.

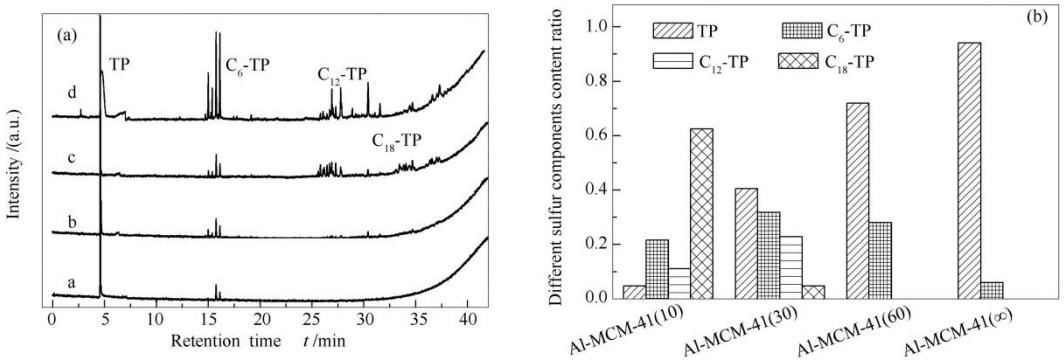

Figure10 GC-SCDchromatograms (a)anddifferentsulfidesdistributionmap(b)ofextractionsolutionsbyAl-MCM-41sample

a:Al-MCM-41(∞);b:Al-MCM-41(60);c:Al-MCM-41(30);d:Al-MCM-41(10)

3. Conclusion

Al-MCM-41 and Molecular Sieve, with high dispersity of aluminum species prepared by post grafting method and maintained regular two-dimensional hexagonal pore structure. When the amount of aluminum species introduced is low, easily forms tetra-coordinated form, B, acid center and tri-coordinated form, L_1 type acid center ; when the amount of aluminum species introduced is high, easily forms penta-coordinated form, L_2 type acid center. The three acid centers all have adsorption effects on thiophene sulfides. The adsorption capacity of L_2 type acid center is obviously stronger than L_1 type acid center, L_1 type acid center is slightly stronger than B and acid center, so the L_2 type acid center in pentacoordinate form is the ideal thiophene adsorption active site alkene and thiophene undergo competitive adsorption and catalytic conversion reactions on b and acid centers, and catalytic conversion reactions dominate. L_2 existence of acid center can obviously improve B Catalytic conversion reaction on acid center. Macromolecular sulfide generated by catalytic conversion replaces thiophene to be adsorbed on the active center, which significantly improves the saturated sulfur adsorption capacity of molecular sieve.

References

1. Mao Yanhong, Liu Dongmei,Wang Haiyan,Wang Yujia. Basic Acid Modification ZSM-5 Studyon Thiophene Alkylation Performance of Molecular Sieve Catalyst [J]. Journal of Fuel Chemistry, 2017, 45(12):1456－1466.
2. DEHGHANR, ANBIAM. Zeolitesforadsorptivedesulfurizationfromfuels:Areview[J]. Fuel Process Technol, 2017,

167:99－116.
3. SONGCS. Anoverviewofnewapproachestodeepdesulfurizationforultra-cleangasolinedieselfuelandjetfuel[J]. CatalToday, 2003, 86(1): 211－263.
4. ZHOUAN, MAXLSONGCS. Effects of oxidative modification of carbon surface on the adsorptionofsulfurcompoundsindieselfuel[J]. ApplCatalB: Environ, 2009, 87: 190－199.
5. Wang Hongguo,Heng Jiang,Xu Jing,Sun Zhaolin, Zhang Xiaotong, Zhu Heli, Song Lijuan. Benzene and 1- Octene Effect on Ce (IV) Y Molecular Sieve Selective Adsorption Desulfurization [J]. Journal of Physical Chemistry, 2008, 24(9): 1714－1718.
6. DUANLH, GAOXH, MENGXH, ZHANGHT, WANGQ, QINYC, ZHANGXT, SONGLJ. Adsorption, co-adsorption, andreactionsofsulfurcompounds, aromatics, olefinsover Ce-exchangedYZeolite[J]. JPhysChemC, 2012, 116(49):25758－25756.
7. Song Lijuan, Hu Yueting, Qin Yucai, Wen Guang, Zhang Xiaotong. NiY and Study on Mechanism of Influence of Surface Acidity of Molecular Sieve on Its Selective Adsorption Desulfurization Performance [J] . Journal of Fuel Chemistry , 2016, 44(9):1082－1088.
8. ZUY, QINYC, GAOXH, LIUHH, ZHANGXT, ZHANGJD, SONGLJ. Insightintothe correlationbetweentheadsorption-transformationbehaviorsofmethylthiophenesandtheactivesitesofzeolitesY[J]. ApplCatalB:Environ, 2017, 203:96－107.
9. Wang Wangyin, Pan Mingxue, Qin Yucai ,Wang Lingtao ,Song Lijuan . Cu (I) Y Effect of Surface Acidity of Molecular Sieve on Its Adsorption Desulfurization Performance [J] . Journal of Physical Chemistry , 2011, 27(5):1176－1180.
10. SCHALLMOSERS, HALLERGL, SANCHEZ-SANCHEZM, LERCHERJA. Roleof spatialconstraintsofBrnstedacidsitesforadsorptionandsurfacereactionsoflinearpentenes[J]. JAmChemSoc, 2017, 139(25):8646－8652.
11. RICHARDEAUD, JOLYG, CANAFFC, MAGNOUXP, GUISNETM, THOMASM, NICOLAOSA. Adsorptionandreactionover HFAUzeolitesof thiopheneinliquidhydrocarbon solutions[J]. ApplCatalA:Gen, 2004, 263(1):49－61.
12. SHIYC, ZHANGW, ZHANGHX, TIANFP, JIACY, CHENYY. Effectof cyclohexene on thiopheneadsorptionoverNaYandLaNaYzeolites[J]. FuelProcessTechnol, 2013, 110:24－32.
13. SELVARAJM, LEETG.Roomtemperaturesynthesisofdiphenylmethane overnovel mesoporous Lewisacidcatalysts[J]. JMolCatal:AChem, 2006, 243(2):176－182
14. WANGZC, JIANGYJ, LAFONO, TREBOSCJ, KIMKD, STAMPFC, BAIKERA, AMOUREUSJ-PHUANGJ. Brnstedacidsitesbasedonpenta-coordinatedaluminumspecies[J]. NatCommun, 2016, 7:13820.
15. HUW, LUOQ, SUYC, CHENL, YUEY, YECH, DENGF. Acidsitesinmesoporous Al-SBA-1 materialas revealed bysolid-stateNMRspectroscopy[J]. MicroporousMesoporousMater, 2006, 92(1):22－30.
16. GURINOVAA, ROZHKOVAYA, ZUKALA, CEJKAJ, SHENDEROVICHIG. Mutablelewis and Br nstedacidityofaluminatedSBA-15asrevealedbyNMR ofadsorbedpyridine-15N[J]. Langmuir, 2011, 27(19):12115.
17. TANGK, SONGLJ, DUANLH, LIXQ, GUIJZ, SUNZL. Deepdesulfurizationby selective adsorptiononaheteroatomszeolitepreparedbysecondarysynthesis[J]. FuelProcessTechnol, 2008, 89(1):1－6.
18. Qin Yucai, High Strength, Pei Tingting, Zheng Lange, Wang Lin, Mo Zhousheng, Song Lijuan. Study on Adsorption and Catalytic Transformation of Thiophene on Rare Earth Ion Modified Y Type Molecular Sieves [J] . Journal of Fuel Chemistry , 2013, 41(7):889－896.
19. ZhangChang ,Qin Yucai ,High Strength ,Zhang Haitao ,Mo Zhou Sheng ,Early Spring Rain ,Zhang Xiaotong ,Song Lijuan . Modulation Mechanism of Ce Modification on Acidity and Catalytic Conversion Performance of Y-Type Molecular Sieves [J]. Journal of Physical Chemistry , 2015, 31(2):344－352.
20. Zuyun ,Qin Yucai ,High Strength ,Mo Zhou Sheng ,Zhang Lei ,Zhang Xiaotong ,Song Lijuan . thiophene and modification under catalytic cracking conditions y mechanism of action of molecular sieve [j] . Journal of Fuel Chemistry , 2015, 43(7):862－869.
21. Ding Rundong ,Zuyun ,Zhou Chuanxing ,Wang Huan ,Mo Zhousheng ,Qin Yucai ,Sun Zhaolin ,Song Lijuan . CuNaY, Study on the Correlation between Effective Adsorption Sites of Molecular Sieves and Their Desulfurization Performance [J] . Journal of Fuel Chemistry , 2018, 46(4):451－458.
22. DUBD, ROYRS, ONDT, BELANDF, KALIAGUINES. Aluminumchloridegrafted mesoporousmolecularsievesasalkylationcatalysts[J]. MicroporousMesoporousMater, 2005, 79:137－144.
23. GALLOJMR, BISIOC, GATTIG, MARCHESEL, PASTOREHO. Physicochemical charac terizationandsurfaceacidpropertiesofmesoporous[Al]-SBA-15obtainedbydirectsynthesis[J]. Langmuir, 2010, 26(8):5791－5800.
24. MARQUESJP, GENERI, AYRAULTP, BORDADOJC, LOPESJM, RIBEIROFR, GUISNETM. Infraredspectroscopicstudyoftheacidpropertiesofdealuminated BEAzeolites[J]. MicroporousMesoporousMater, 2003, 60:251－262.
25. EMIESCA. Determinationofintegratedmolarextinction coefficientsforinfraredabsorption bandsofpyridineadsorbedonsolidacidcatalyst[J]. JCatal, 1993, 141:347－354.